MULTI-PHYSICS LATTICE DISCRETE PARTICLE MODEL (M-LDPM) FOR THE COUPLING OF DIFFUSION PROCESSES AND FRACTURE

EMI Conference 2024
Chicago, IL
May 29, 2024

Hao Yin, Matthew Treomner, Weixin Li, Erol Lale, Mohammed Alnaggar, Lifu Yang, Lei Shen, Giovanni Di Luzio, and Gianluca Cusatis

Northwestern | McCORMICK SCHOOL OF ENGINEERING

Carbon neutral: CO_2 emissions

- CO_2 emissions, are of primary resources of greenhouse gas emissions, influence the global climate change.
- Construction industry, is responsible for up to 10% of total CO_2 emissions per year (ACI, 2018).
- According to the *Paris Agreement*, the major carbon emitters need to cut the emission to limit global warming “well below” 1.5 ℃ (2.7 ℉) of current level.

Figure 1: CO_2 emissions and global climate change [1]

[1] Credit: https://www.azocleantech.com/news.aspx?newsID=31271

Carbon neutral: durability & sustainability

- A key factor which will lessen the environmental footprint of building materials is improving the durability and sustainability.
- A comprehensive understanding of the multiphysical phenomena will be vital to ensure an optimal life-cycle of the structure, and the minimization of environmental impacts.

Figure 2: Concrete chloride attack [2]

Figure 3: Crumbing concrete driveway [3]

[2] Credit: https://www.giatecscientific.com/education/service-life-prediction-for-reinforced-concrete-exposed-to-chloride-induced-corrosion-risk/
[3] Credit: https://gfpcement.com/correcting-concrete-3-signs-need-repair-work

Multiphysics-LDPM framework

- The Lattice Discrete Particle Model (LDPM) has proved its efficiency on simulating softening and fracture of quasi-brittle materials such as concrete, shale, etc., while the Flow Lattice Model (FLM), a topologically dual lattice model of LDPM, has been proposed for diffusion/flow problems.

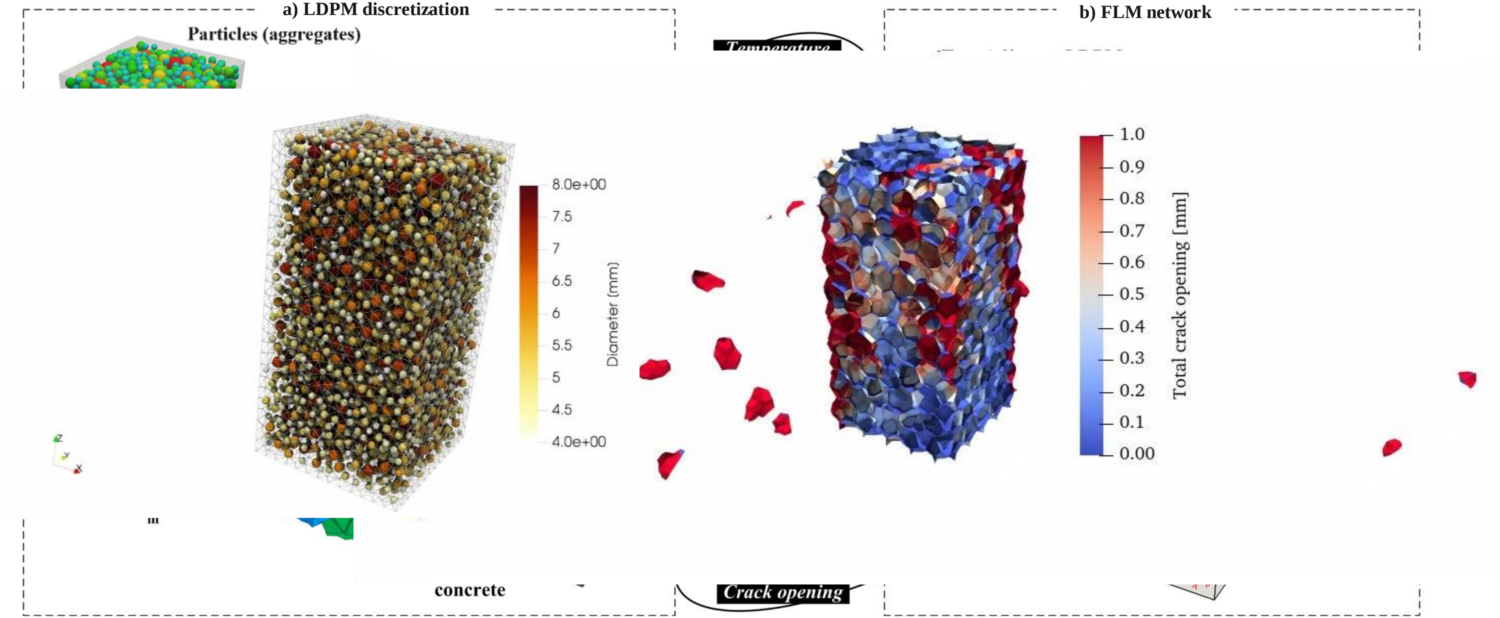

Figure 4: LDPM-FLM coupling framework setup: a) LDPM discretization, b) FLM network (adopted from [4])

[4] Image credit: Shen, Lei, et al. "Multiphysics lattice discrete particle model for the simulation of concrete thermal spalling." *Cement and Concrete Composites* 106 (2020): 103457.

Multiphysics-LDPM framework

- The Lattice Discrete Particle Model (LDPM) has proved its capability on simulating softening and fracture of quasi-brittle materials such as concrete, shale, etc., while the Flow Lattice Model (FLM), a topologically dual lattice model of LDPM, has been proposed for diffusion/flow problems.

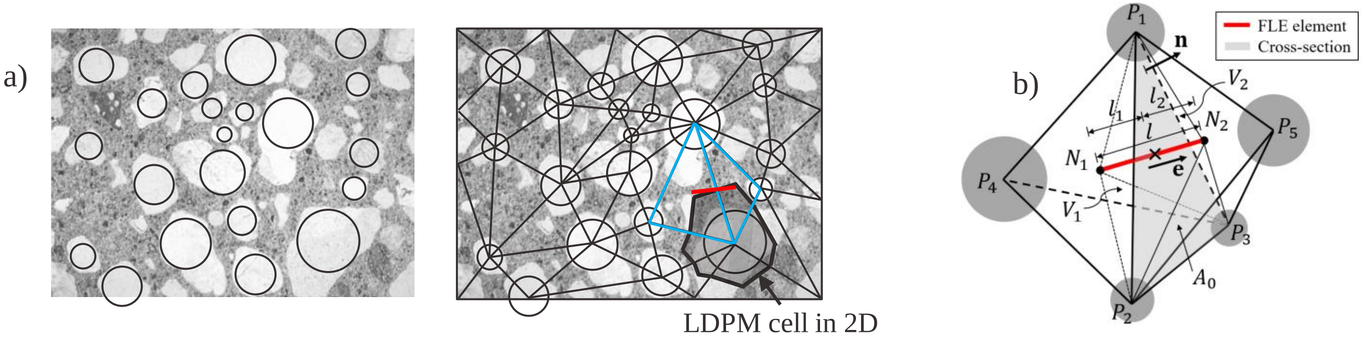

Figure 5: LDPM and the *Flow Lattice Model* setup: a) concrete mesostructure and LDPM tessellation in 2D, b) conduit Flow Lattice element in association with adjacent LDPM tetrahedra in 3D

Flow lattice element formulation – saturated flow

- Balance equation in each control volume V_I associated with node N_I [5]:

$$V_I C(p_I)\dot{p}_I + Aj = V_I S(p_I) \qquad I \in 1,2 \qquad (1)$$

Fick's first law of diffusion governs the diffusion flux density:

$$j = -\xi(p)\frac{\partial p}{\partial x} \qquad (2)$$

The discrete estimation of gradient between N_1 and N_2 reads:

$$\frac{\partial p}{\partial x} = \frac{\Delta p}{l}\mathbf{e} = \frac{p_1 - p_2}{l}\mathbf{e} \qquad (3)$$

The discretized balance equation for flow lattice element:

$$\begin{cases} V_1 C(p_1)\dot{p}_1 - A\xi(\bar{p})\dfrac{p_2 - p_1}{l} = V_1 S(p_1) & (4a) \\ V_2 C(p_2)\dot{p}_2 + A\xi(\bar{p})\dfrac{p_2 - p_1}{l} = V_2 S(p_2) & (4b) \end{cases}$$

weighted average $\bar{p} = \frac{V_2 p_1 + V_1 p_2}{V_1 + V_2}$

A- area associated with j

$A = A_0 \mathbf{e} \cdot \mathbf{n}$

l- FLE length

C - capacity

S - source/sink term

ξ- permeability

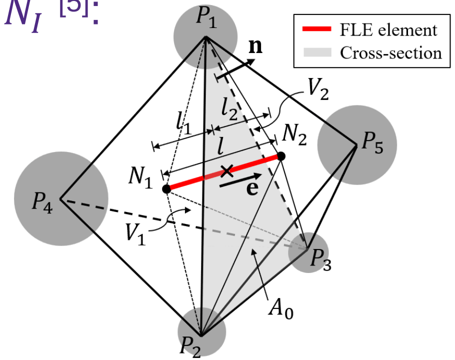

Figure 6: Flow Lattice Element (FLE) geometry in 3D

Let $C_1 = C(p_1), C_2 = C(p_2), \xi = \xi(\bar{p}), S_1 = S(p_1)$, $S_2 = S(p_2)$:

$$\mathbf{u} = [p_1 \;\; p_2]^{\mathrm{T}} \qquad \mathbf{f} = \mathbf{M}\dot{\mathbf{u}} + \mathbf{K}\mathbf{u} - \mathbf{S} = \mathbf{0}$$

$$\begin{bmatrix} V_1 C_1 & 0 \\ 0 & V_2 C_2 \end{bmatrix}\dot{\mathbf{u}} + \frac{A}{l}\begin{bmatrix} \xi & -\xi \\ -\xi & \xi \end{bmatrix}\mathbf{u} - \begin{bmatrix} V_1 S_1 \\ V_2 S_2 \end{bmatrix} = \mathbf{0} \qquad (5)$$

[5] Credit: Li, W., Zhou, X., Carey, J.W., Frash, L.P. and Cusatis, G., 2018. Multiphysics lattice discrete particle modeling (M-LDPM) for the simulation of shale fracture permeability. *Rock Mechanics and Rock Engineering, 51*, pp.3963-3981.

Coupled fracture-flow analysis

- Coupled fracture-flow governing equation in the FLM [6]:

$$\mathbf{u} = [p_1 \;\; p_2]^{\mathrm{T}} \qquad \mathbf{f} = \mathbf{M}\dot{\mathbf{u}} + \mathbf{K}\mathbf{u} - \mathbf{S} = \mathbf{0}$$

$$\begin{bmatrix} V_1 C_1 & 0 \\ 0 & V_2 C_2 \end{bmatrix} \dot{\mathbf{u}} + \frac{A}{l} \begin{bmatrix} \xi & -\xi \\ -\xi & \xi \end{bmatrix} \mathbf{u} - \begin{bmatrix} V_1 S_1 \\ V_2 S_2 \end{bmatrix} = \mathbf{0}$$

where $C_i = M_b^{-1} + V_{ci}(K_f V_i)^{-1}$

$V_{ci} = \sum_{j=1}^{3} A_{fj}^i \, \delta_{Nj}^i$ cracked volume

$$\xi = \frac{\bar{\rho}_f (\kappa_0 + \kappa_c)}{\rho_{f0} \mu_f}$$

$\kappa_c = \frac{1}{12A}\left(\frac{g_2}{I_{c1}} + \frac{g_1}{I_{c2}}\right)^{-1}$ $\quad I_{ci} = \sum_{j=1}^{3} l_{fj}(\delta_{Nj}^i)^3$

$$S_i = b\dot{\varepsilon}_{Vi} + \rho_{fi} \dot{V}_{ci} (\rho_{f0} V_i)^{-1}$$

$\dot{\varepsilon}_{Vi} = \frac{\varepsilon_{Vi_{t+\Delta t}} - \varepsilon_{Vi_t}}{\Delta t}$ rate of volumetric strain

$\dot{V}_{ci} = \frac{V_{ci_{t+\Delta t}} - V_{ci_t}}{\Delta t}$ rate of cracked volume

p_i - nodal pore pressure ($i = 1{,}2$)
V_i - uncracked control volume

M_b - Biot modulus of the porous media
K_f - fluid bulk modulus

$\bar{\rho}_f$ - average fluid density
κ_0 - intrinsic permeability of the porous media
κ_c - permeability of the cracked volume according to 2D Poiseuille flow
μ_f - fluid viscosity

$\dot{\varepsilon}_{Vi}$ - rate of volumetric strain
b - Biot coefficient

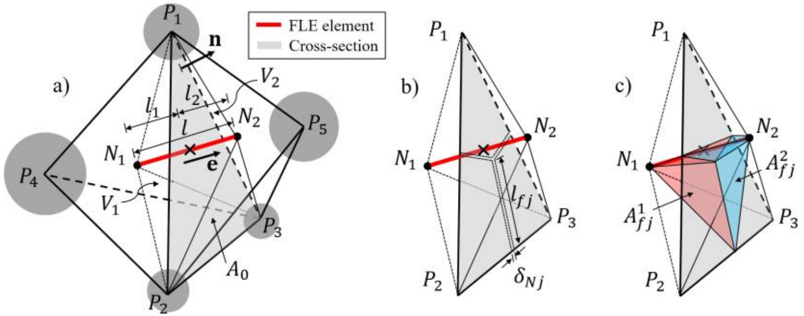

[6] Ref: Rice, James R., and Michael P. Cleary. "Some basic stress diffusion solutions for fluid-saturated elastic porous media with compressible constituents." *Reviews of Geophysics* 14.2 (1976): 227-241.

Multiphysics problems in LDPM-FLM framework

- Different meshes, different time scales of the coupled-fields complicate the coupling process (a.k.a. "multidomain" or "multimodel" coupling).

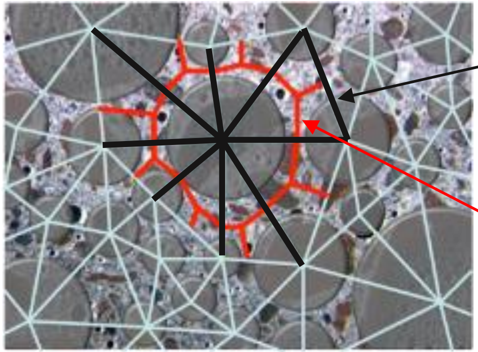

Figure 7: LDPM tessellation and the FLM system in 2D [7]

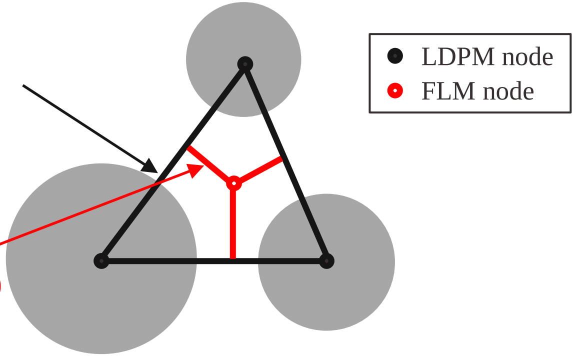

Figure 8: Schematics of the dual lattices in 2D

- Fully-coupled approaches ✖ (solving equations concurrently)
- Sequential approaches { spatial mapping / temporal mapping }

[7] Credit: Li, Weixin. *Computational and experimental characterization of the behaviors of anisotropic quasi-brittle materials: Shale and textile composites*. Diss. Northwestern University, 2018.

Two-way coupling between solvers

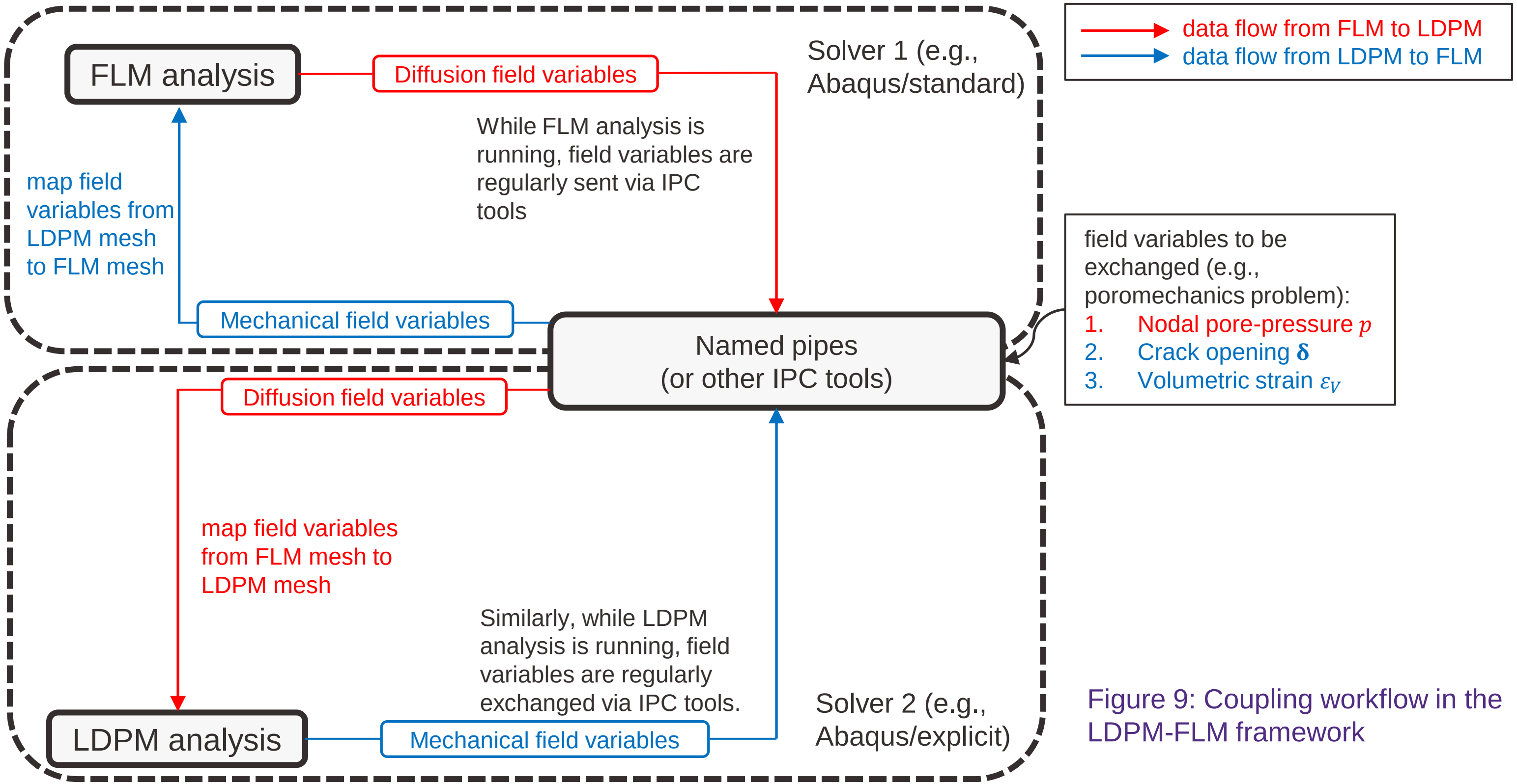

Figure 9: Coupling workflow in the LDPM-FLM framework

Two-way coupling between solvers

- The LDPM-FLM coupling framework uses the Inter-process communication (IPC) tools for the data-exchange between solvers.
  - For UNIX-based systems (Linux, NU Quest) – named pipes

- Coupling scheme:

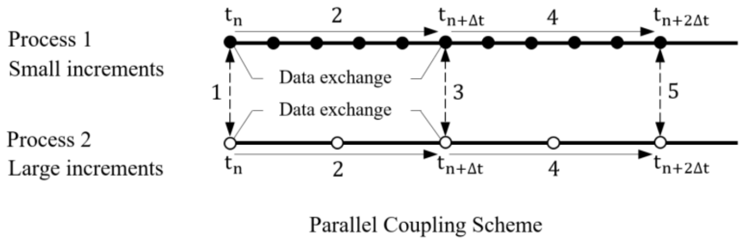

Figure 10: Parallel coupling scheme used in the LDPM-FLM framework

- Time incrementation scheme:

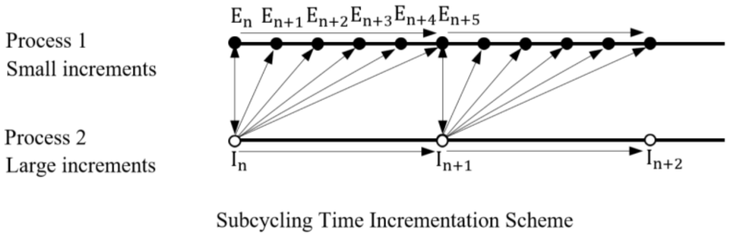

Figure 11: Time incrementation scheme used in the LDPM-FLM framework

- In Abaqus implementations, the algorithms were embedded in Fortran user subroutines.

Two-way Coupling: Verification

- Benchmark 1: poroelasticity problem, 1D Terzaghi's consolidation.

Effective facet normal stress:

$$\bar{\sigma}_N = \sigma_N + \sigma_N^p = f(\varepsilon_N, \varepsilon_T, \dots)$$

$$\sigma_N^p = -bp$$

Imposed stress (σ_N^p)

Biot's coefficient (b)

Source/sink term caused by the mechanical volume change:

$$S_i = b\dot{\varepsilon}_{Vi}$$

Rate of volumetric strain ($\dot{\varepsilon}_{Vi}$)

Biot's coefficient (b)

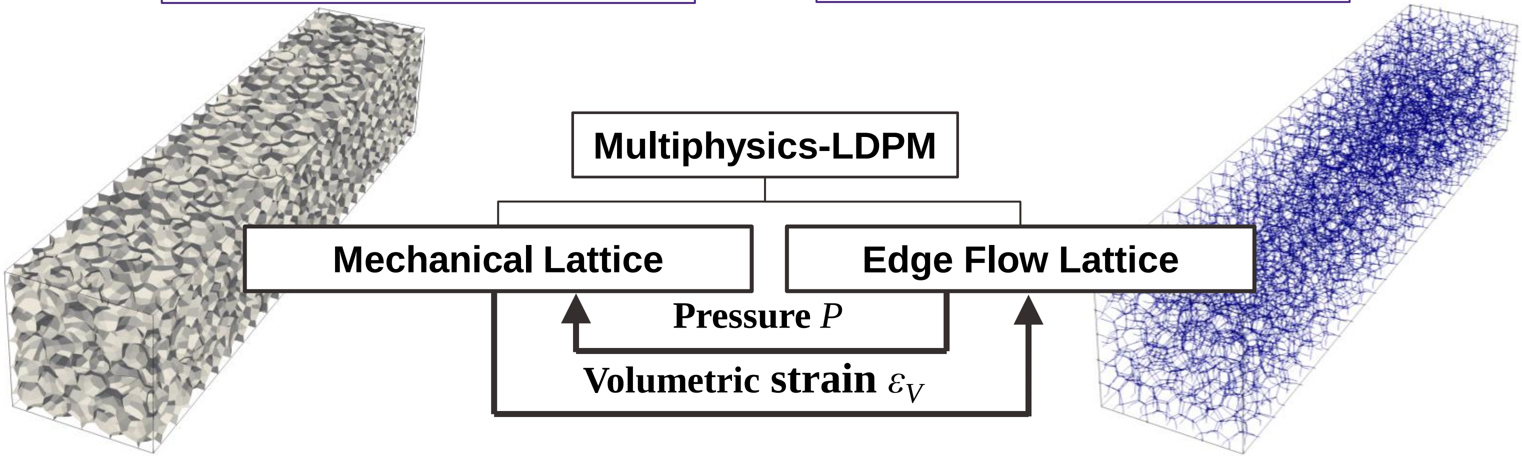

Figure 12: Setup for the two-way coupled, 1D Terzaghi's consolidation problem

Two-way Coupling: Verification

- Benchmark 1: 1D Terzaghi's consolidation.

Analytical solution [8]:

loading by pressure $p(\chi,\tau) = p^{\star} F_1(\chi,\tau)$ $\quad u(\chi,\tau) = -\dfrac{p^{\star}\Upsilon L}{G} F_2(\chi,\tau)$

where:

$$F_1(\chi,\tau) = 1 - \sum_{m=1,3,\ldots}^{\infty} \frac{4}{m\pi} \sin\left(\frac{m\pi\chi}{2}\right) \exp\left(-m^2\pi^2\tau\right) \quad F_2(\chi,\tau) = \sum_{m=1,3,\ldots}^{\infty} \frac{8}{m^2\pi^2} \cos\left(\frac{m\pi\chi}{2}\right) \left[1 - \exp\left(-m^2\pi^2\tau\right)\right]$$

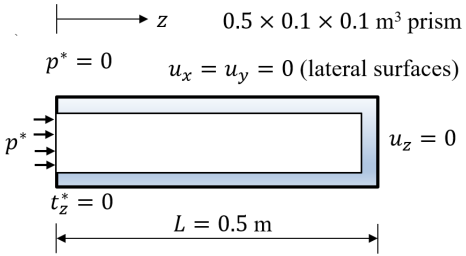

$$\chi = \frac{x}{L} \qquad \tau = \frac{\lambda t}{4CL^2} \qquad \Upsilon = \frac{b(1-2\nu)}{2(1-\nu)}$$

$$G = \frac{E}{2(1+\nu)} \qquad C = \frac{(1-\nu_u)(1-2\nu)}{M_b(1-\nu)(1-2\nu_u)} \qquad M_b = \frac{1}{c}$$

$$\nu_u = \frac{3K_u - 2G}{2(3K_u + G)} \qquad K_u = M_b b^2 + \frac{E}{3(1-2\nu)}$$

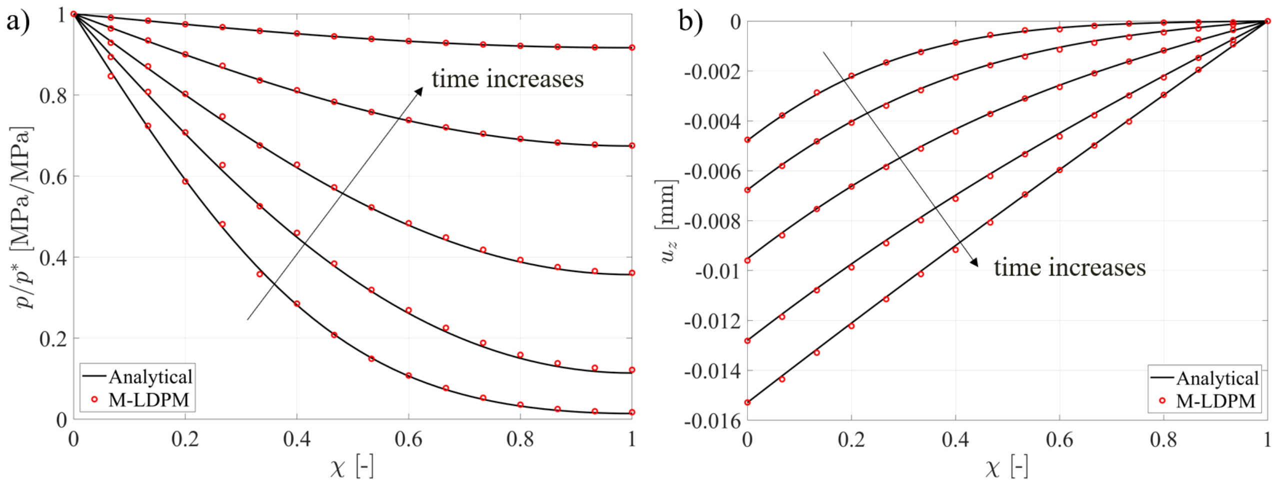

Figure 13: Simulation results of 1D Terzaghi's consolidation: a) dimensionless pressure profile and b) axial expansion profile at various stages

[8] Ref: Detournay, Emmanuel, and Alexander H-D. Cheng. "Fundamentals of poroelasticity." *Analysis and design methods*. pergamon, 1993. 113-171.

Two-way Coupling: Verification

- Benchmark 2: poroelasticity problem, radial expansion in a thick-walled hollow cylinder due to fluid injection.

Effective facet normal stress

$$\bar{\sigma}_N = \sigma_N + \sigma_N^p = f(\varepsilon_N, \varepsilon_T, \dots)$$

$$\sigma_N^p = -bp$$

Imposed stress

Biot's coefficient

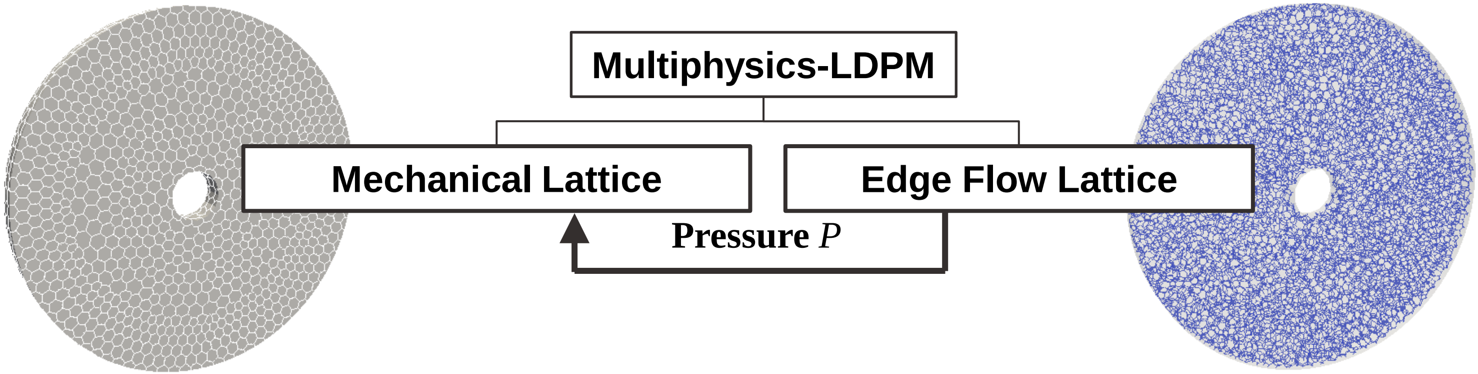

Figure 14: Setup for the one-way coupled, poroelastic radial expansion problem

Two-way Coupling: Verification

- Benchmark 2: poroelasticity problem, radial expansion in a thick-walled hollow cylinder due to fluid injection.

Analytical solution [9]: $\bar{u} = -b\bar{P}_{fi}\frac{1-\nu^2}{2}\left[\frac{\bar{r}_o^2}{\bar{r}_o^2-1}\left(\frac{1+\nu}{1-\nu}\frac{1}{\bar{r}}+\bar{r}\right)+\bar{r}\frac{\frac{1}{1+\nu}-\ln\bar{r}}{\ln\bar{r}_o}\right]-(1-b)\bar{P}_{fi}\frac{\bar{r}_o^2}{\bar{r}_o^2-1}\left(\frac{1+\nu}{\bar{r}}+\frac{\bar{r}(1-\nu)}{\bar{r}_o^2}\right)$

and $P_f = P_{fi}\frac{\log\frac{r_o}{r}}{\log\frac{r_o}{r_i}}$ where: $\bar{u} = \frac{u}{r_i}$ $\bar{r} = \frac{r}{r_i}$ $\bar{r}_o = \frac{r_o}{r_i}$ $\bar{P}_f = \frac{P_f}{E_c}$ $\bar{P}_{fi} = \frac{P_{fi}}{E_c}$ $E_c = \frac{2+3\alpha}{4+\alpha}E_0$ $\nu = \frac{1-\alpha}{4+\alpha}$

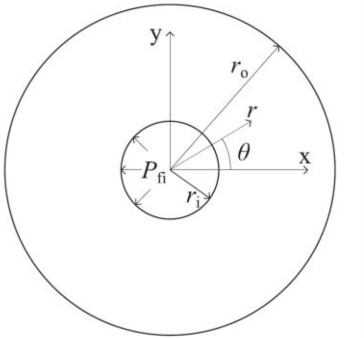

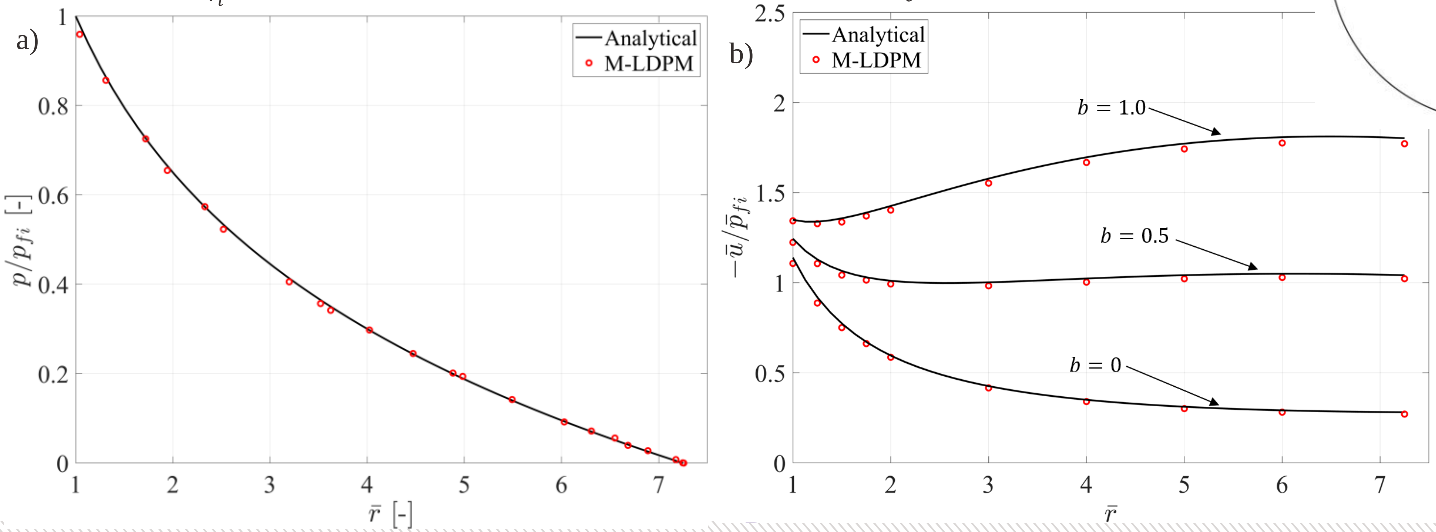

Figure 15: Simulation results of poroelastic expansion: a) dimensionless pressure profile at steady-state, b) dimensionless radial expansion profiles with various Biot's coefficients

[9] Ref: Grassl, Peter, et al. "On a 2D hydro-mechanical lattice approach for modelling hydraulic fracture." *Journal of the Mechanics and Physics of Solids* 75 (2015): 104-118.

Two-way Coupling: Verification

- Benchmark 3: hydraulic fracturing of hollow thick-walled cylinder due to fluid injection.

Effective facet normal stress

$$\bar{\sigma}_N = \sigma_N + \sigma_N^p = f(\varepsilon_N, \varepsilon_T, \dots)$$

$$\sigma_N^p = -bp$$

Imposed stress

Biot's coefficient

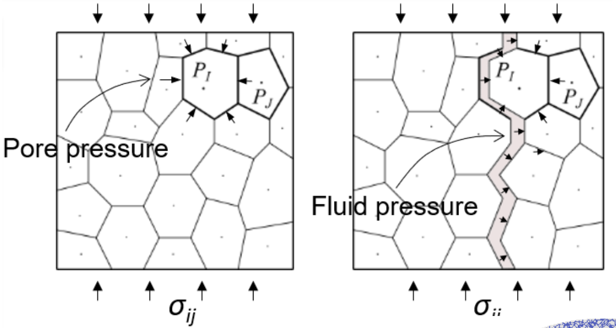

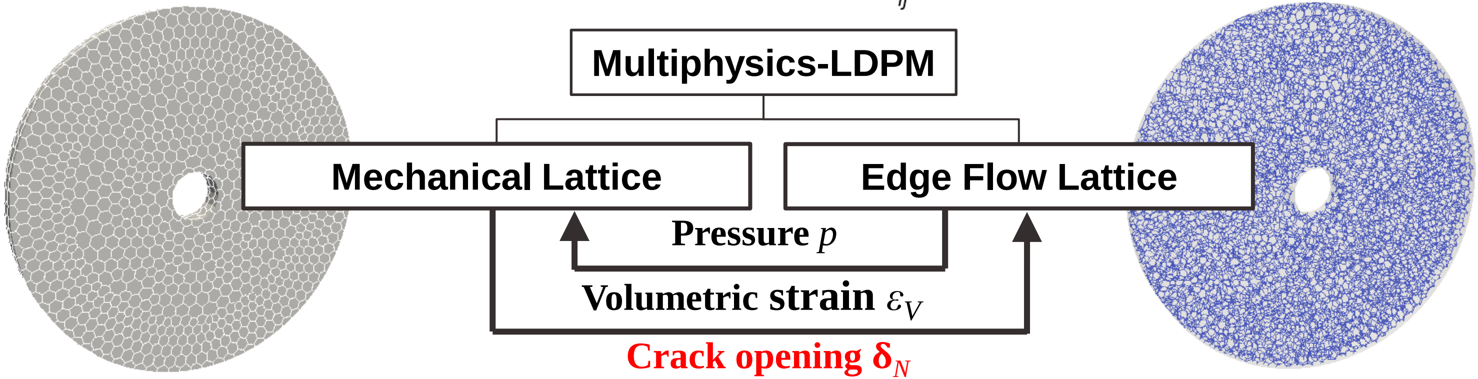

Figure 16: Setup for the two-way coupled, hydraulic fracturing problem

Two-way Coupling: Verification

- Benchmark 3: hydraulic fracturing of hollow thick-walled cylinder due to fluid injection.

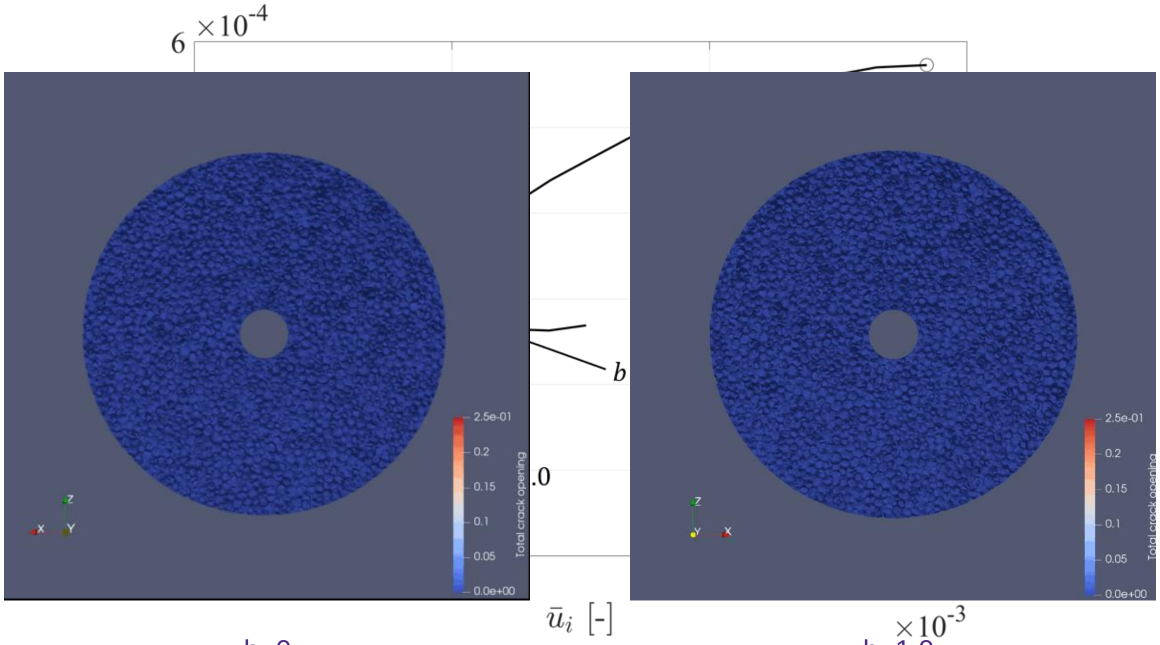

Figure 17: Simulation results of hydraulic fracturing: dimensionless pressure vs. dimensionless radial displacement at the inner boundary of the hollow cylinder

Two-way Coupling: Verification

- Benchmark 3: hydraulic fracturing of hollow thick-walled cylinder due to fluid injection.

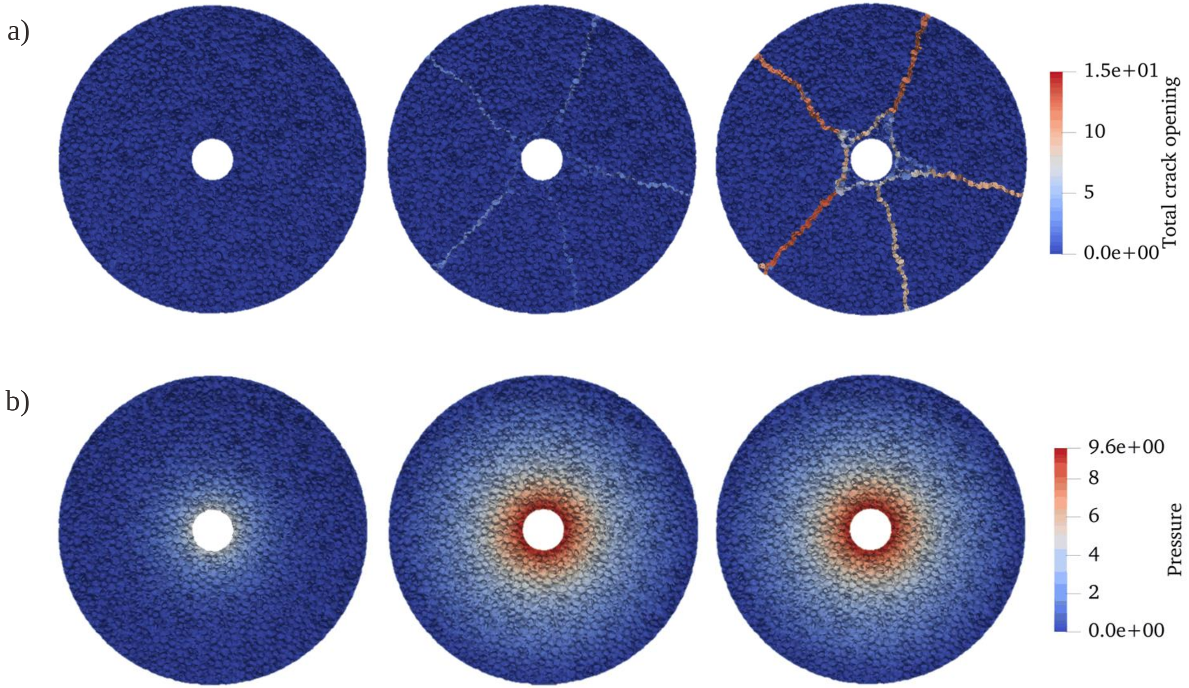

Figure 18: a) Crack patterns (crack opening contours) and b) pressure contours for uncoupled condition at three moments marked in Fig. 37

Two-way Coupling: Verification

- Benchmark 3: hydraulic fracturing of hollow thick-walled cylinder due to fluid injection.

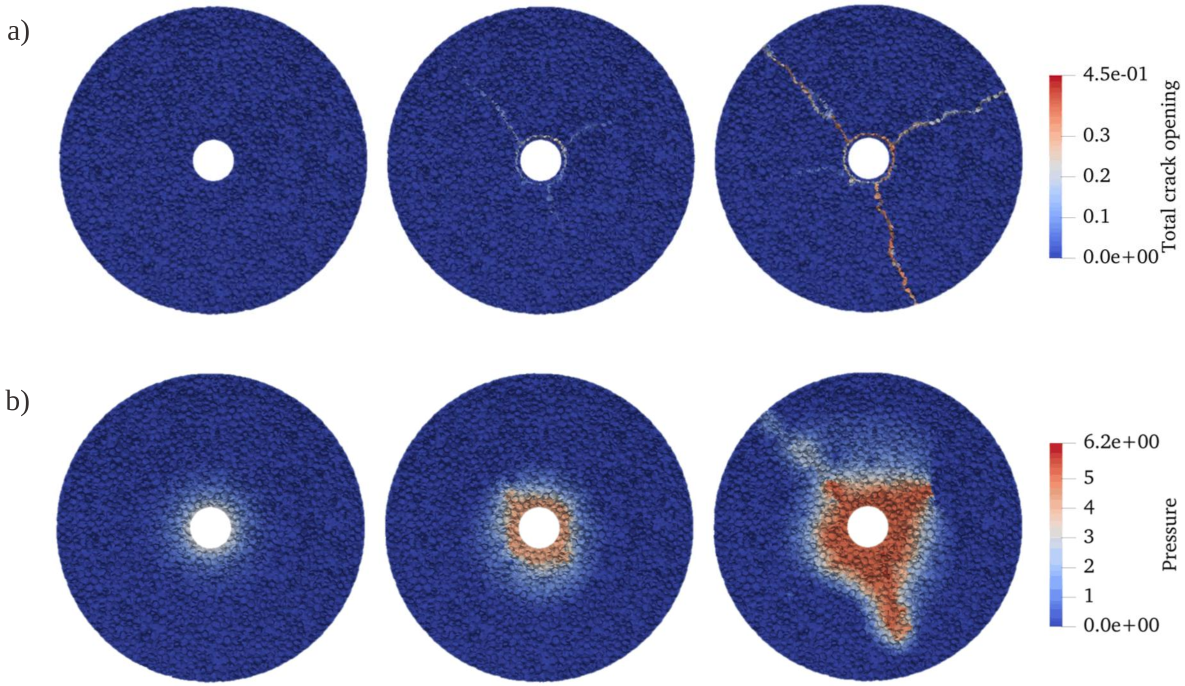

Figure 19: a) Crack patterns (crack opening contours) and b) pressure contours for fully-coupled condition ($b = 1.0$) at three moments marked in Fig. 37

Summary

- A multiphysics framework for Lattice Discrete Particle Model (LDPM)-Flow Lattice Model (FLM) coupling has been developed.
- The multiphysics framework is capable to solve poroflow (poroelasticity, hydraulic fracturing) problems accurately.
- The coupled analysis shows the effects of Biot’s coefficients on the crack pattern, as well as the pressure diffusion in hydraulic fracturing.

Suggested work

- Extend the multiphysics framework for the coupling with more physical fields (e.g., temperature, chemical, biochemical components).
- Incorporate the parallel computing in the multiphysics framework to improve the efficiency.

Questions?

Northwestern | McCORMICK SCHOOL OF ENGINEERING

Topologically dual lattices

- The topological duality (e.g., Voronoi-Delaunay duality), has been brought to describe many coupled physical phenomena, such as aligned cracks and conduit elements allowing to accurately reflect the crack opening effect on the flow.

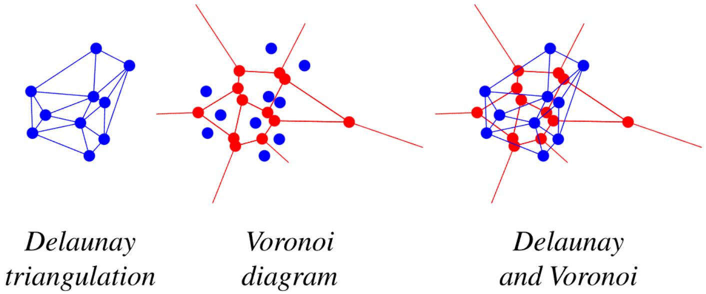

Figure 5: Voronoi-Delaunay duality [5]

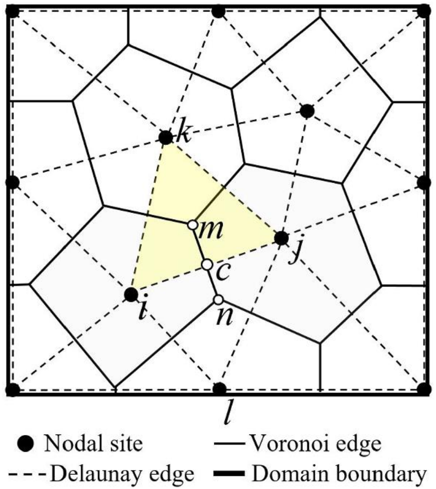

Figure 6: A 2D dual lattices using the concept of Voronoi-Delaunay duality [6]

[5] Credit: https://mathworld.wolfram.com/DelaunayTriangulation.html.
[6] Credit: Hwang, Young Kwang, et al. "Compatible coupling of discrete elements and finite elements using Delaunay–Voronoi dual tessellations." *Computational Particle Mechanics* 9.6 (2022): 1351-1365.

Application: hygro-thermal-chemical evolution in fresh concrete

- The discrete implementation of the HTC model (Di Luzio and Cusatis 2009):

Hygro-Thermo-Chemical

$$W_I \frac{\partial w_e}{\partial H} \dot{H}_I + S^* j_H = W_I q_H \qquad (6a)$$

$$W_I \rho c_T \dot{T}_I + S^* j_T = W_I q_T \qquad (6b)$$

$$I \in P, Q$$

w_e - evaporable water content
ρ - concrete density
c_T - specific heat of concrete
S^* - area associated with j
D_H - moisture permeability
κ - heat conductivity
q_H - moisture source/sink term
q_T - heat source/sink term

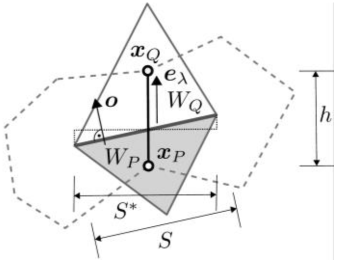

The moisture and heat flux density are governed by an equivalent Darcy's law and Fourier's law, respectively:

$$j_H = -D_H(H,T) \frac{\partial H}{\partial x} \quad (7) \qquad\qquad j_T = -\kappa \frac{\partial T}{\partial x} \quad (8)$$

The discretized balance equation for flow lattice element PQ:

$$\begin{cases} W_P \frac{\partial w_e}{\partial H}(H_P, T_P)\dot{H}_P - S^* D_H(\bar{H}, \bar{T}) \frac{H_Q - H_P}{l} = W_P q_H(H_P, T_P) & (9a) \\ W_P \rho c_T \dot{T}_P - S^* \kappa \frac{T_Q - T_P}{l} = W_P q_T(H_P, T_P) & (9b) \\ W_Q \frac{\partial w_e}{\partial H}(H_Q, T_Q)\dot{H}_Q + S^* D_H(\bar{H}, \bar{T}) \frac{H_Q - H_P}{l} = W_Q q_H(H_Q, T_Q) & (9c) \\ W_Q \rho c_T \dot{T}_Q + S^* \kappa \frac{T_Q - T_P}{l} = W_Q q_T(H_Q, T_Q) & (9d) \end{cases}$$

Let $C_P = \frac{\partial w_e}{\partial H}(H_P, T_P), C_T = \rho c_T, C_Q = \frac{\partial w_e}{\partial H}(H_Q, T_Q)$,
$\bar{D}_H = D_H(\bar{H}, \bar{T}), q_{HI} = q_H(H_I, T_I), q_{TI} = q_T(H_I, T_I)$:

$$\mathbf{u} = [H_P \; T_P \; H_Q \; T_Q]^{\mathrm{T}} \qquad \mathbf{f} = \mathbf{M}\dot{\mathbf{u}} + \mathbf{K}\mathbf{u} - \mathbf{S} = \mathbf{0}$$

$$\begin{bmatrix} W_P C_P & 0 & 0 & 0 \\ 0 & W_P C_T & 0 & 0 \\ 0 & 0 & W_Q C_Q & 0 \\ 0 & 0 & 0 & W_Q C_T \end{bmatrix} \dot{\mathbf{u}} + \frac{S^*}{l} \begin{bmatrix} \bar{D}_H & 0 & -\bar{D}_H & 0 \\ 0 & \kappa & 0 & -\kappa \\ -\bar{D}_H & 0 & \bar{D}_H & 0 \\ 0 & -\kappa & 0 & \kappa \end{bmatrix} \mathbf{u} - \begin{bmatrix} W_P q_{HP} \\ W_P q_{TP} \\ W_Q q_{HQ} \\ W_Q q_{TQ} \end{bmatrix} = \mathbf{0}$$

Coupling between solvers

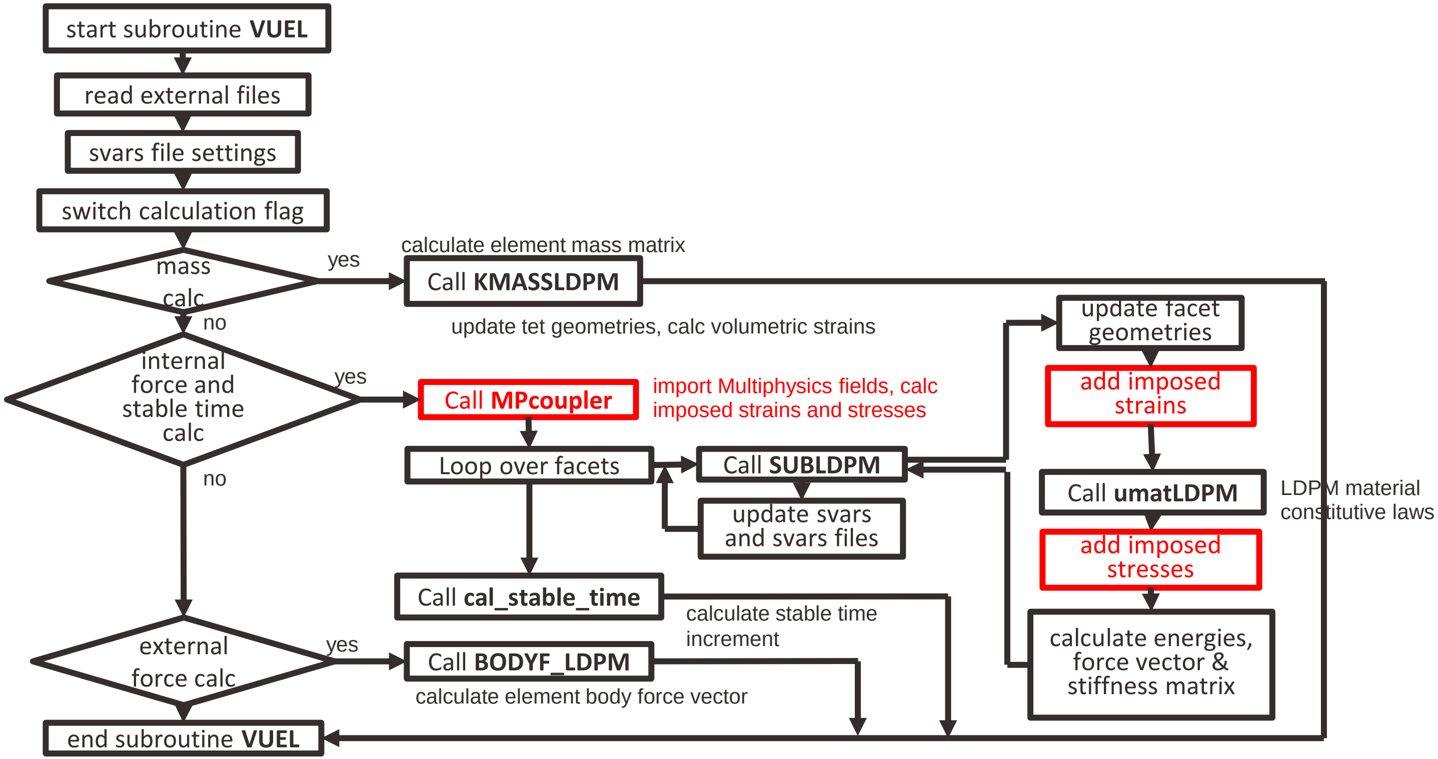

Coupling between solvers

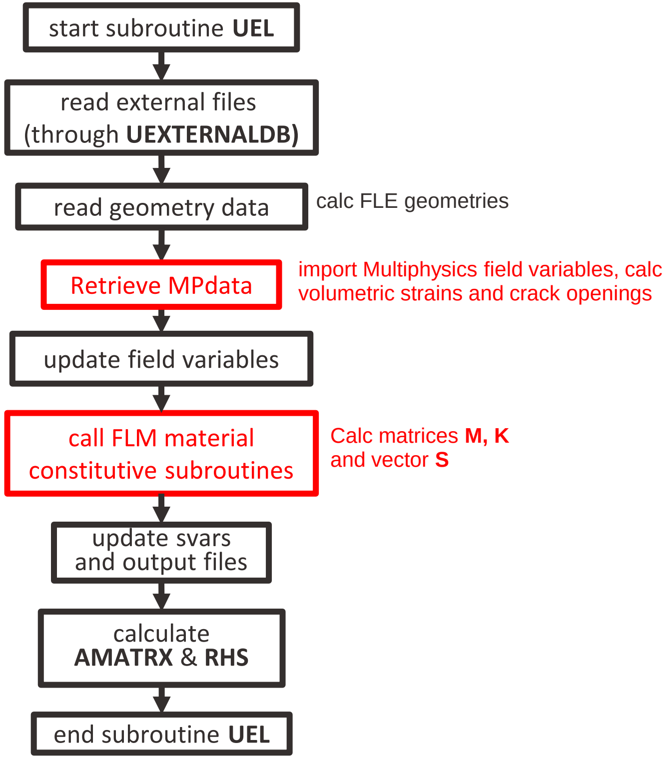

Coupling between solvers

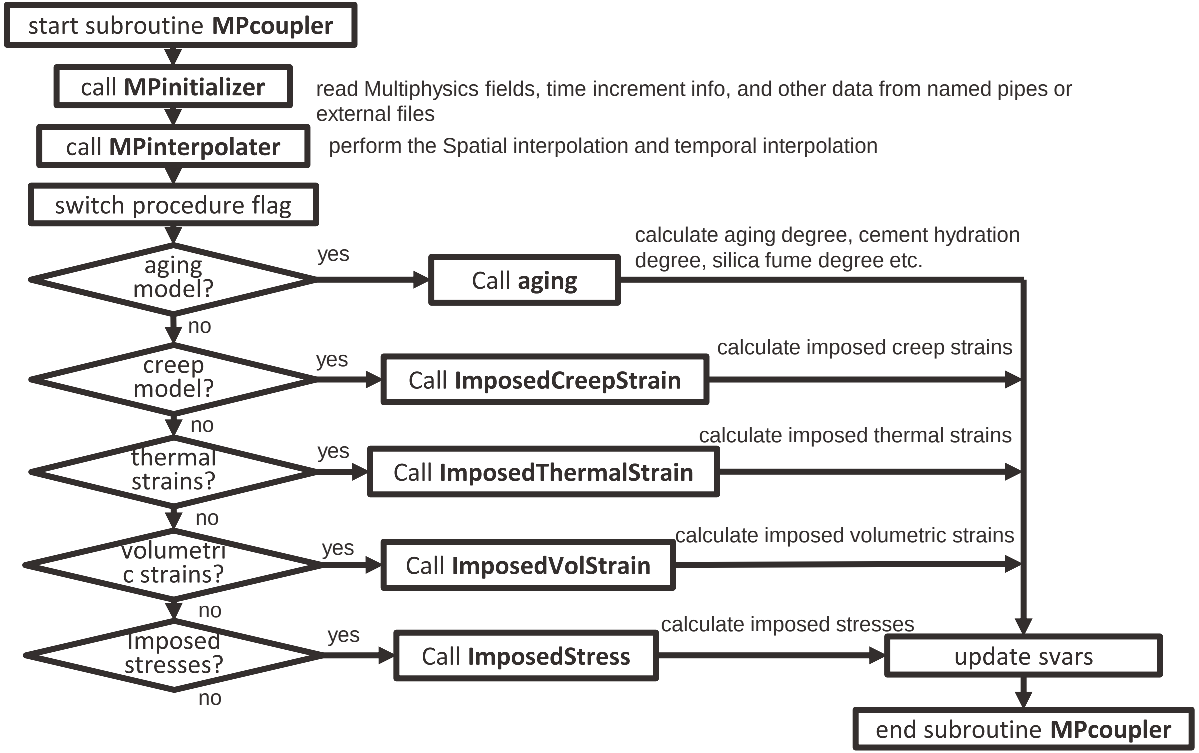

FLM Application: hygro-thermo-chemical evolution in fresh concrete

- Governing equation for HTC problem (Di Luzio and Cusatis 2009 paper [2] or detailed derivation):

$$V_1\left(\frac{\partial w_e}{\partial h}\dot{h} + \frac{\partial w_e}{\partial T}\dot{T} + \frac{\partial w_e}{\partial \alpha_c}\dot{\alpha}_c + \frac{\partial w_e}{\partial \alpha_s}\dot{\alpha}_s + \dot{w}_n\right) + AD_h\frac{h_2 - h_1}{l}\mathbf{e}\cdot\mathbf{n} = 0$$

$$V_1\left(\rho c_t \dot{T} + \dot{\alpha}_s s \tilde{Q}_s^{\infty} + \dot{\alpha}_c c \tilde{Q}_c^{\infty}\right) + A\lambda\frac{T_2 - T_1}{l}\mathbf{e}\cdot\mathbf{n} = 0$$

$$V_2\left(\frac{\partial w_e}{\partial h}\dot{h} + \frac{\partial w_e}{\partial T}\dot{T} + \frac{\partial w_e}{\partial \alpha_c}\dot{\alpha}_c + \frac{\partial w_e}{\partial \alpha_s}\dot{\alpha}_s + \dot{w}_n\right) - AD_h\frac{h_2 - h_1}{l}\mathbf{e}\cdot\mathbf{n} = 0$$

$$V_2\left(\rho c_t \dot{T} + \dot{\alpha}_s s \tilde{Q}_s^{\infty} + \dot{\alpha}_c c \tilde{Q}_c^{\infty}\right) - A\lambda\frac{T_2 - T_1}{l}\mathbf{e}\cdot\mathbf{n} = 0$$

$$\mathbf{f} = \mathbf{M}\dot{\mathbf{u}} + \mathbf{K}\mathbf{u} - \mathbf{S} = \mathbf{0} \qquad \mathbf{u} = [h_1 \ \ T_1 \ \ h_2 \ \ T_2]^{\mathrm{T}}$$

$$V_w\begin{bmatrix} g_1C_1 & g_1C_2 & 0 & 0 \\ g_1C_3 & g_1C_4 & 0 & 0 \\ 0 & 0 & g_2C_1 & g_2C_2 \\ 0 & 0 & g_2C_3 & g_2C_4 \end{bmatrix}\dot{\mathbf{u}} + \frac{A_w}{l}\begin{bmatrix} D_1 & D_2 & -D_1 & -D_2 \\ D_3 & D_4 & -D_3 & -D_4 \\ -D_1 & -D_2 & D_1 & D_2 \\ -D_3 & -D_4 & D_3 & D_4 \end{bmatrix}\mathbf{u} - V_w\begin{bmatrix} g_1S_1 \\ g_1S_2 \\ g_2S_1 \\ g_2S_2 \end{bmatrix} = \mathbf{0}$$

Linearization with Newton-Raphson, let $\mathbf{f}(\mathbf{u}_{n+1}) \approx \mathbf{f}(\mathbf{u}_n) + \frac{\partial \mathbf{f}(\mathbf{u}_n)}{\partial \mathbf{u}}\Delta\mathbf{u} = \mathbf{0}$

$$\frac{\partial \mathbf{f}(\mathbf{u}_n)}{\partial \mathbf{u}}\Delta\mathbf{u} = -\mathbf{f}(\mathbf{u}_n)$$

Use $-\mathbf{f}(\mathbf{u}_n) = -(\mathbf{M}\dot{\mathbf{u}}_n + \mathbf{K}\mathbf{u}_n - \mathbf{S})$ as RHS

$\frac{\partial \mathbf{f}(\mathbf{u}_n)}{\partial \mathbf{u}}$ as tangent stiffness (AMATRX)

[2] Credit: Di Luzio, G. and Cusatis, G., 2009. Hygro-thermo-chemical modeling of high performance concrete. I: Theory. *Cement and Concrete composites, 31*(5), pp.301-308.

Two-way coupling between solvers

- The mechanical analysis is done in Abaqus/Explicit, implemented with the Abaqus user-defined element VUEL, the transport analysis is done in Abaqus/Standard, implemented with Abaqus user-defined element UEL.

- The core functionality – sequential coupling between two Abaqus solvers is achieved through data communication interface in FORTRAN subroutines.

```fortran
C=====================================================================C
C     Two-way coupling processes
C=====================================================================C
      call VGETOUTDIR(OUTDIR,LENOUTDIR)    ! Work directory

      if (kstep == 0) then ! Abaqus/Explicit Packager stage
        ! if (Lop /= 0) then ! Second call of VUEL subroutine in Abaqus/Explicit Packager stage
          ! continue
        ! end if
        continue
      else ! Abaqus/Explicit Analysis stage
        if (kinc == 0) then ! Initial data exchange settings
          if (tetID == nomaxel) then ! Exchange when loop to the last element
            ! Sending LDPM info to Abaqus/Standard solver
            open(V2U,file='LDPM2FLM.pipe',defaultfile=trim(OUTDIR),form='formatted',
     1           status='old',action='write',access='stream')
            write(*,*) 'Sending LDPM analysis settings'
            write(V2U,'(I8)') nomaxel
            write(V2U,'(ES24.17)') period
            flush(V2U)
            close(V2U)

            ! Receiving FLM info from Abaqus/Standard solver
            open(U2V,file='FLM2LDPM.pipe',defaultfile=trim(OUTDIR),form='formatted',
     1           status='old',action='read',access='stream')
            write(*,*) 'Retriving FLM analysis settings'
            read(U2V,'(I8)') nnode_FLM
            write(*,*) "nnode_FLM", nnode_FLM
            read(U2V,'(I8)') MPtypeFLM
            write(*,*) "MPtypeFLM", MPtypeFLM

            close(U2V)

            if (MPtypeFLM == 1) then
              nfieldFLM = 2
            else if (MPtypeFLM == 2) then
              nfieldFLM = 1
            end if

            if (allocated(FLM2LDPM_DATA) == 0) then
              allocate(FLM2LDPM_DATA(nnode_FLM,nfieldFLM),LDPM2FLM_DATA(nomaxel,13))
              allocate(FLM2LDPM_DATA_old(nnode_FLM,nfieldFLM))
              LDPM2FLM_DATA = 0.0d0
              FLM2LDPM_DATA = 0.0d0
              FLM2LDPM_DATA_old = 0.0d0
            end if
          end if
```

Figure 12: Data communication interface in FORTRAN subroutines

FLM Application: hygro-thermo-chemical evolution in fresh concrete

- Relative humidity and temperature evolution in a newly-constructed concrete dam

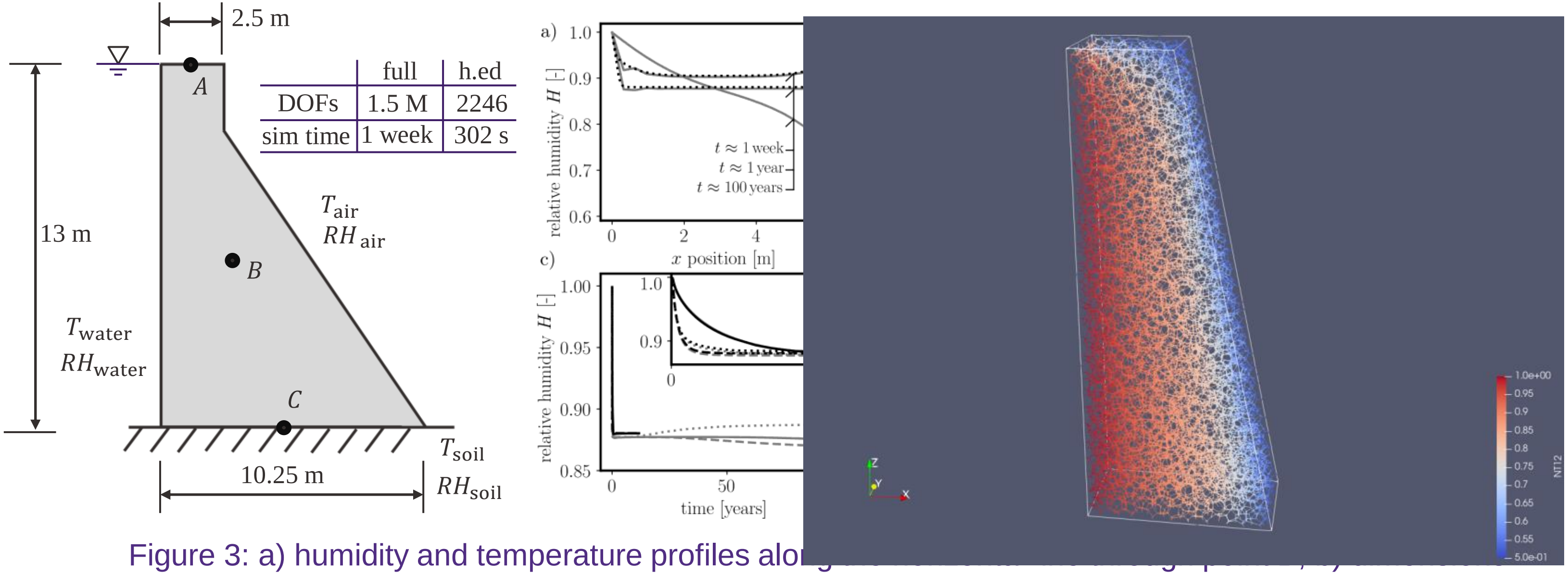

	full	h.ed
DOFs	1.5 M	2246
sim time	1 week	302 s

Figure 3: a) humidity and temperature profiles alo… and boundary conditions, c) evolution of humidity, temperature and cement hydration degree at points A, B, and C (Compared with the homogenized model in Eliáš et al. 2022 [3])

[3] Credit: Eliáš, Jan, Hao Yin, and Gianluca Cusatis. "Homogenization of discrete diffusion models by asymptotic expansion." *International Journal for Numerical and Analytical Methods in Geomechanics* 46.16 (2022): 3052-3073.